Title:
IRE1α and TRB3 do not contribute to the disruption of proximal insulin signaling caused by palmitate in C2C12 myotubes

Names of authors:
Nicolas Pierre[1], Rodrigo Fernández-Verdejo[1], Pauline Regnier[1], Simon Vanmechelen[1], Bénédicte Demeulder[1], Marc Francaux[1]

Author affiliation:
[1]Institute of Neuroscience, Université catholique de Louvain, Louvain-la-Neuve, Belgium

Running title:
Uncoupling of UPR and insulin signaling

Corresponding author:
Prof. Marc Francaux, PhD
Place Pierre de Coubertin -1, bte L8.10.01
1348 Louvain-la-Neuve
Belgium
Phone: +32-10-474457
Fax: +32-10-472093
marc.francaux@uclouvain.be

Keywords:
ER stress; insulin resistance; JNK; muscle; UPR

Abbreviations:
ATF4: activating transcription factor 4; BiP: binding immunoglobulin protein; CHOP: C/EBP homologous; eEF2: eukaryotic elongation factor 2; ER: endoplasmic reticulum; GRP94: 94 kDa glucose-regulated protein; IR: insulin resistance; IRE1α: inositol-requiring 1α; IRS-1: insulin receptor substrate 1; JNK: c-Jun N-terminal kinase; NEFA: non-esterified fatty acids; OL: oleate; PA: palmitate; PPIA: peptidylprolyl isomerase A; RPL4: ribosomal protein L4; RPL19: ribosomal protein L19; Sc: scramble; TRB3: tribbles homolog 3; UPR: unfolded protein response; XBP1: X-box-binding protein 1

Abstract

Endoplasmic reticulum (ER) stress is a central actor in the physiopathology of insulin resistance (IR) in various tissues. The subsequent unfolded protein response (UPR) interacts with insulin signaling through inositol-requiring 1α (IRE1α) activation and tribbles homolog 3 (TRB3) expressions. IRE1α impairs insulin actions through the activation of c-Jun N-terminal kinase (JNK) and TRB3 is a pseudokinase inhibiting Akt. In muscle cells, the link between ER stress and IR has only been demonstrated by using chemical ER stress inducers or overexpression techniques. However, the involvement of ER stress in lipid-induced muscle IR remains controversial. The aim of the study was to test whether palmitate-induced IRE1α signaling and TRB3 expression disturb insulin signaling in myogenic cells. C2C12 myotubes were exposed to palmitate and then stimulated with insulin. siRNA transfection was used to downregulate TRB3 and IRE1α. Palmitate increased TRB3 expression, activated IRE1α signaling and reduced the insulin-dependent Akt phosphorylation. Knocking down TRB3 or IRE1α did not prevent the inhibitory effect of palmitate on Akt phosphorylation. Our results support the idea that ER stress is not responsible for lipid-induced IR in C2C12 myotubes.

1. Introduction

Insulin resistance (IR) is associated with obesity, a pathological state in which energy excess is stored as fat. It is well established that lipid excess impairs insulin-stimulated glucose disposal. Although many researches have been conducted, the mechanism by which non-esterified fatty acids (NEFA) induce IR remains unclear. Lately, endoplasmic reticulum (ER) has appeared as a key actor in this pathological process (Ozcan et al. , 2004, Ozcan et al. , 2006).

In addition to its functions in lipid biosynthesis, calcium storage and protein folding, ER plays a major role in the sensing, integration and response to numerous cellular stresses (Cnop et al. , 2012).

ER is a vast network of cisterns, where secreted and transmembrane proteins are folded. Cells modulate both the quantity of nascent proteins and the folding capacity to maintain ER proteostasis. Physiological or pathological conditions generating an imbalance between protein load and folding capacity lead to an accumulation of unfolded proteins into the ER, a state known as ER stress. To cope with this stress, cells trigger a homeostatic response called unfolded protein response (UPR). In mammalian cells, UPR is activated by three sensor proteins: inositol-requiring 1α (IRE1α), doublestranded RNA-dependent protein kinase (PKR)-like ER kinase and activating transcription factor 6. Under homeostatic conditions, the binding immunoglobulin protein (BiP) is associated with the luminal domain of the sensors. Upon ER stress, BiP dissociates from them, thus activating their downstream signaling. The UPR coordinates an adaptive response in three steps: 1) translational inhibition of protein synthesis; 2) transcriptional upregulation of ER stress-inducible genes coding for ER-resident chaperones, ER-export proteins and ER-associated protein degradation components; 3)

apoptosis if the previous responses are not sufficient to restore ER homeostasis (Zhang and Kaufman, 2008).

UPR activation has been demonstrated to alter insulin signaling. Two mechanisms have been proposed: 1) IRE1α signaling leads to c-Jun N-terminal kinase (JNK) activation, which subsequently inhibits the insulin receptor substrate 1 (IRS-1) (Ozcan et al. , 2004); 2) UPR upregulates the expression of tribbles homolog 3 (TRB3), which is a pseudokinase that inhibits Akt and IRS-1 (Du et al. , 2003, Ohoka et al. , 2005, Koh et al. , 2013). However, the involvement of these mechanisms in muscle IR is still controversial. In ob/ob mice, attenuation of ER stress by chemical chaperone injection improves insulin sensitivity in skeletal muscle (Ozcan et al. , 2006). On the contrary, the use of chemical chaperones does not prevent palmitate-induced IR in C2C12 myotubes (Hage Hassan et al. , 2012).

Given the controversy, we used a different approach to deal with the issue. We knocked down IRE1α or TRB3 in C2C12 myotubes before palmitate exposure. Then, the Akt response to insulin was assessed. The aim of the study was to test whether IRE1α-JNK pathway and TRB3 participate to the disturbance of insulin signaling caused by palmitate in C2C12 myotubes.

2. Materials and methods

2.1. Cell culture

C2C12 mouse myoblasts (ATCC) were seeded in 6-well plates (1.10^5 cells/well) and cultured at 37 °C in a humidified incubator containing 5% CO_2. Cells grew in a high glucose (4.5 g/L) Dulbeccos's Modified Eagle Medium (DMEM, Life Technologies) supplemented with 10% (v/v) fetal bovine serum, 100 U/ml penicillin and 100 µg/ml streptomycin (Life Technologies). When cells reached confluence (48 h), medium was replaced by a

differentiation medium containing DMEM, 2% (v/v) horse serum (Lonza), 100 U/ml penicillin and 100 µg/ml streptomycin. After 96 h, C2C12 myotubes were incubated for 17 h with palmitate, oleate or the corresponding vehicle. To investigate the insulin pathway, C2C12 myotubes were stimulated with 100 nM insulin (Actrapid, Novo Nordisk) for 10 minutes.

2.2. NEFA preparation

Palmitate and oleate (Sigma-Aldrich) were dissolved in ethanol to 100 mM. These NEFA solutions were diluted to 1 mM in a differentiation medium supplemented with 2% (w/v) low endotoxin bovine serum albumin (Sigma-Aldrich) and filtered through a 0.2 µm porosity filter (Sarstedt). The molar ratio of fatty acid to albumin was 3.3.

2.3. Western blotting

Cells were washed twice with cold phosphate-buffered saline (PBS), and then harvested in ice-cold lysis buffer [20 mM Tris, 270 mM sucrose, 5 mM EGTA, 1 mM EDTA, 0.1% Triton X-100, 1 mM sodium orthovanadate, 50 mM sodium β-glycerophosphate, 5 mM sodium pyrophosphate, 50 mM sodium fluoride, 1 mM 1,4-dithiothreitol (DTT), and 10% protease inhibitor cocktail 10X (Roche Applied Science), pH 7.0]. Homogenates were centrifuged at 10,000 *g* for 10 min at 4 °C. Supernatants were immediately stored at -80 °C. Protein concentration was determined using the DC protein assay kit (Bio-Rad) with BSA as standard. Western blots were performed as previously described (Pierre et al. , 2014). Antibodies were from Cell Signaling: IRE1α, phosphorylated-Akt (Ser^{473} and Thr^{308}), Akt, phosphorylated-JNK (Thr^{183}/Tyr^{185}), JNK, phosphorylated-c-Jun (Ser^{73}), c-Jun and eukaryotic elongation factor 2 (eEF2).

2.4. RNA extraction and quantitative Real-time PCR

Total RNA was extracted with Trizol® (Life Technologies) according to manufacturer's instructions. The RNA purity and quantity were assessed with Nanodrop® spectrophotometer (Isogen). Reverse transcription was performed with iScript cDNA synthesis kit (Bio-Rad) from 1 µg total RNA. Real time PCR experiments were done on a MyIQ2 thermocycler (Bio-Rad) using the following conditions: 3 min at 95 °C, followed by 40 cycles of 30 s at 95 °C, 30 s at 60 °C and 30 s at 72 °C. Samples were analyzed in duplicate in a 10 µl reaction volume containing 4.8 µl IQSybrGreen SuperMix (Bio-Rad), 0.1 µl of each primer (200 nM final concentration) and 5 µl of cDNA. Primers sequences are reported in Table 1. Melting curves were systematically analyzed to ensure the specificity of the amplification. Target genes were normalized using three reference genes according to the geNorm analysis (Vandesompele et al. , 2002). The reference genes were ribosomal protein L19 (RPL19), peptidylprolyl isomerase A (PPIA) and ribosomal protein L4 (RPL4).

2.5. RNA interference

The on-target smart pools interfering RNA for TRB3, IRE1α and scramble were from Dharmacon (Thermo Scientific). After 24 h of differentiation, cells were transfected with Lipofectamin® RNAiMax (Life Technologies) and 50 nM siRNA for 72 h according to manufacturer's instructions.

2.6. Statistical analysis

All results were expressed relatively to the control group and presented as means ± SEM. Three independent cultures were used. In each culture, duplicates or triplicates were used. Differences between two means were assessed using two-tailed unpaired t-test. Data

involving more than two groups were analysed with either one-way or two-way ANOVA as appropriate. Bonferroni post-hoc test was used. A P-value <0.05 was considered significant.

3. Results

3.1. Palmitate induces ER stress and disrupts insulin signaling

Firstly, we aimed to confirm the ER stress induction by palmitate. We measured the mRNA level of several ER stress markers in C2C12 myotubes incubated with palmitate or oleate. Upon ER stress, the UPR-inducible genes activating transcription factor 4 (ATF4) and C/EBP homologous (CHOP) cooperate to induce TRB3 transcription (Ohoka et al. , 2005). Consistent with this regulation, palmitate increased transcripts of ATF4 (3-fold, P<0.001), CHOP (19-fold, P<0.001) and TRB3 (20-fold, P<0.001) (Figure 1A). When activated by ER stress, IRE1α splices an mRNA encoding for the X-box-binding protein 1 (XBP1). In our experiments, the mRNA level of the spliced form of XBP1 (XBP1s) increased by 20-fold (P<0.001) after incubation with palmitate (Figure 1A). XBP1s is then translated into a potent bZIP transcription factor, which regulates the ER-resident chaperones BiP and the 94 kDa glucose-regulated protein (GRP94) (Malhotra and Kaufman, 2007). Our results showed that palmitate increased the transcript level of BiP (16-fold, P<0.001) and GRP94 (6-fold, P<0.001) (Figure 1A). All together, these results confirm that palmitate induces ER stress in C2C12 myotubes. On the other hand, incubation with oleate did not induce any modification of the ER stress markers (Figure 1A).

Secondly, we wanted to corroborate the disruption of insulin signaling caused by palmitate in C2C12 myotubes. We incubated cells with palmitate or oleate and then measured the changes in phospho-Akt induced by insulin. Insulin increased the phosphorylation state of Akt-Ser^{473} (277%, P<0.001) and Akt-Thr^{308} (287%, P<0.05) (Figure 1B). As expected,

palmitate reduced Akt-Ser^{473} and Akt-Thr^{308} phosphorylations in both basal (69% and 81%, respectively) and insulin-stimulated conditions (71% and 85%, respectively) (Figure 1B). In contrast, oleate did not affect Akt phosphorylations in either basal or insulin-stimulated conditions (Figure 1B).

3.2. TRB3 does not contribute to palmitate-induced impairment of insulin signaling

In C2C12 myotubes, palmitate-induced Akt inhibition was associated with TRB3 expression (Figure 1). Thus, we tested whether TRB3 was responsible for the altered Akt response. To this end, we knocked down TRB3 with siRNA. siRNA reduced the basal level of TRB3 mRNA (72%, $P<0.01$) and its upregulation induced by palmitate (66%, $P<0.01$) (Figures 2A and 2B). Unfortunately, the protein level of TRB3 was undetectable despite the use of three commercial antibodies tested with positive controls (not shown).

C2C12 myotubes were incubated with palmitate in the presence of scramble or TRB3 siRNA and then stimulated with insulin. As a control of cells responsiveness after the transfection procedure, scramble transfected myotubes were stimulated with insulin. As expected, insulin increased phospho-Akt-Ser^{473} (101%, $P<0.001$) and phospho-Akt-Thr^{308} (181%, $P<0.01$) (Figures 2C, 2D and 2E). In the scramble siRNA condition, palmitate reduced Akt-Ser^{473} and Akt-Thr^{308} phosphorylations in both basal state (67% and 68%, respectively) and after insulin stimulation (56% and 63%, respectively). The same responses were found in the TRB3 siRNA condition (Figures 2C, 2D and 2E).

3.3. IRE1α does not participate in palmitate-induced impairment of insulin signaling

To test the implication of IRE1α on palmitate-induced IR, we downregulated this protein with siRNA. IRE1α protein level became undetectable after IRE1α siRNA transfection (Figure 3C). In addition, palmitate upregulated IRE1α protein level, this response was

drastically reduced by IRE1α siRNA (Figure 3C). To check whether IRE1α knockdown was sufficient to reduce its activation, we measured the product of IRE1α activation, i.e., XBP1s mRNA. In the basal state, XBP1s mRNA was reduced by 82% ($P<0.001$) with IRE1α siRNA (Fig. 3A). As expected, XBP1s mRNA was upregulated by palmitate (16-fold) and addition of IRE1α siRNA reduced this effect (66%, $P<0.001$) (Fig. 3B). Consequently, IRE1α activation was efficiently reduced by the siRNA.

To evaluate the link between IRE1α and JNK, we measured JNK activation after palmitate incubation, with or without IRE1α siRNA. The phosphorylation state of both JNK and its downstream target, c-Jun, were used as markers of JNK activation. Palmitate did not alter JNK phosphorylation (Figures 3D and 3F). However, palmitate did increase phospho-c-Jun level, thus suggesting JNK activation (Figures 3E and 3F). The increase of phospho-c-Jun was attenuated by IRE1α siRNA (Figures 3E and 3F). These results indicate that palmitate exposure leads to IRE1α-dependent JNK activation in C2C12 myotubes.

Since IRE1α-JNK pathway was activated by palmitate, we tested its effect on insulin signaling by using IRE1α siRNA. Palmitate-induced IRE1α protein expression was efficiently blocked by the siRNA (Figure 3I). As expected, in the scramble condition, palmitate reduced phospho-Akt-Ser^{473} and phospho-Akt-Thr^{308} levels in both basal (59% and 54%, respectively) and insulin-stimulated conditions (43% and 32%, respectively) (Figures 3G, 3H and 3I). These reductions were independent of IRE1α since its knockdown did not modify the effect (Figures 3G, 3H and 3I).

4. Discussion

By using a downregulation approach, we demonstrated that palmitate-induced IRE1α-JNK signaling and TRB3 expression do not disturb the proximal insulin signaling in C2C12

myotubes. This supports the notion that palmitate-induced IR is not mediated by ER stress in C2C12 myotubes.

In human, dietary intake of saturated NEFA reduce whole-body insulin sensitivity (Vessby et al. , 2001). *In vitro* studies reveal that saturated NEFA, unlike unsaturated, induce IR in muscle cells (Yuzefovych et al. , 2010). We found that palmitate, but not oleate, induced ER stress and altered insulin signaling in C2C12 myotubes. This result is consistent with another report (Salvado et al. , 2013).

Recently, it was proposed that ER stress plays a central role in the development of IR (Eizirik et al. , 2008, Hotamisligil, 2010). This hypothesis might explain the distinct effects of saturated and unsaturated NEFA on insulin signaling observed in our study. At a mechanistic level, ER stress inhibits the insulin pathway mainly through the activation of IRE1α-JNK signaling (Zhang and Kaufman, 2008). In C2C12 myotubes, Hassan et al. (2012) reported that palmitate activates IRE1α and JNK (Hage Hassan et al. , 2012). In our study, we showed that JNK is under the control of IRE1α. Knockdown of IRE1α attenuated the induction of the JNK downstream target, c-Jun, in response to palmitate. This supports the existence of an IRE1α-JNK signaling axis in C2C12 myotubes, as previously shown in other cell types (Urano et al. , 2000, Ozcan et al. , 2004).

Of note, c-Jun phosphorylation induced by palmitate was not temporally accompanied by JNK phosphorylation. This apparent discrepancy could be due to different durations of the phosphorylation state of JNK and c-Jun. In smooth muscle cells, the duration of JNK phosphorylation induced by interleukin-1β is shorter (30 min) than that of c-Jun (> 2 h) (Zhang et al. , 2012). As we analyzed 17 h after palmitate exposure, we may only have observed the long lasting c-Jun phosphorylation.

In our study, although IRE1α knockdown reduced palmitate-induced JNK activation, it did not prevent the inhibitory effect of palmitate on Akt. This suggests that, IR induced by

palmitate does not depend on the IRE1α-JNK pathway in C2C12 myotubes. This idea is supported by another study using muscle-specific JNK1 knockout mice (Pal et al. , 2013). Indeed, those mice were not protected against skeletal muscle or whole body IR induced by HFD.

UPR also promotes the expression of TRB3, which is known to disrupt insulin signaling (Du et al. , 2003, Ohoka et al. , 2005, Koh et al. , 2013). A recent report proposed that TRB3 mediates ER stress-induced insulin resistance in skeletal muscle (Koh et al. , 2013). It was shown that TRB3 increases in muscles of HFD-fed mice and in C2C12 myotubes exposed to palmitate (Koh et al. , 2013). Additionally, TRB3 overexpression in C2C12 myotubes disrupted insulin signaling (Koh et al. , 2013). Nevertheless, the link between NEFA-induced TRB3 expression and IR was not tested. Here, by knocking down TRB3, we suggest that such a link does not exist. We found that TRB3 downregulation did not prevent the inhibitory effect of palmitate on insulin-stimulated Akt phosphorylation. This is consistent with a report showing that mice overexpressing TRB3 in skeletal muscle have normal insulin responses (An et al. , 2014). Interestingly, Koh et al. (2013) reported that TRB3 siRNA does reverse the IR induced by tunicamycin in C2C12 myotubes. The discrepancy with the present study may be due to differences in the ER stress inducer used. Tunicamycin induces a much stronger ER stress than palmitate, does making the comparison inappropriate (Hotamisligil, 2010). Moreover, Iynedjian (2005) reported a lack of action of TRB3 on Akt, casting doubt on the role of TRB3 in IR (Iynedjian, 2005). More studies are needed to clarify the contribution of TRB3 to IR.

In recent years, the role of ER stress in muscle cells IR has been challenged. In C2C12 myotubes, global attenuation of ER stress by chemical chaperones or BiP overexpression fails to prevent palmitate-induced IR (Hage Hassan et al. , 2012, Rieusset et al. , 2012). By using a different technical approach, the present study supports those findings. In complement of

knockdown, overexpression could have been used in our study to investigate IRE1α and TRB3 function. However, we deliberately chose knockdown and not overexpression techniques. We wanted to test whether palmitate-induced insulin resistance was mediated by TRB3 upregulation and/or IRE1α activation. The most appropriate approach to test this hypothesis was to knockdown IRE1α or TRB3 in the presence of palmitate. Indeed, overexpression of TRB3 or IRE1α would involve the absence of palmitate, a condition which does not allow to answer our research question.

Much of the evidence directly linking ER stress to IR has been obtained by using chemical ER stress inducers such as tunicamycin and thapsigargin. However, as those agents induce an extreme level of ER stress, caution must be taken when generalizing the mechanisms unraveled (Hotamisligil, 2010).

We are aware of the limitation inherent to the use of only one cellular model. Accordingly, the conclusions drawn in this article are not generalizable to skeletal muscle. However, to the best of our knowledge, there is no evidence of a different mechanism for the palmitate-induced insulin resistance between C2C12 myotubes and primary skeletal muscle cells.

5. Conclusion

In summary, our results support that palmitate induces ER stress and IR in C2C12 myotubes. The inhibition of insulin-stimulated Akt phosphorylation caused by palmitate was not prevented by the knockdown of IRE1α or TRB3. This suggests no causal relationship between UPR and the proximal insulin signaling in C2C12 myotubes.

Acknowledgements and funding:

This study was granted by the Fonds spéciaux de Recherche (FSR) of the Université catholique de Louvain, RFV is supported by Beca CHILE Doctorado en el Extranjero, convocatoria 2012 and BD by Wagralim, Walloon Region. The authors have no conflict of interest.

References

An D, Lessard SJ, Toyoda T, Lee MY, Koh HJ, Qi L, Hirshman MF, Goodyear LJ. Overexpression of TRB3 in Muscle Alters Muscle Fiber Type and Improves Exercise Capacity in Mice. American journal of physiology Regulatory, integrative and comparative physiology. 2014.

Cnop M, Foufelle F, Velloso LA. Endoplasmic reticulum stress, obesity and diabetes. Trends in molecular medicine. 2012;18:59-68.

Du K, Herzig S, Kulkarni RN, Montminy M. TRB3: a tribbles homolog that inhibits Akt/PKB activation by insulin in liver. Science. 2003;300:1574-7.

Eizirik DL, Cardozo AK, Cnop M. The role for endoplasmic reticulum stress in diabetes mellitus. Endocrine reviews. 2008;29:42-61.

Hage Hassan R, Hainault I, Vilquin JT, Samama C, Lasnier F, Ferre P, Foufelle F, Hajduch E. Endoplasmic reticulum stress does not mediate palmitate-induced insulin resistance in mouse and human muscle cells. Diabetologia. 2012;55:204-14.

Hotamisligil GS. Endoplasmic reticulum stress and the inflammatory basis of metabolic disease. Cell. 2010;140:900-17.

Iynedjian PB. Lack of evidence for a role of TRB3/NIPK as an inhibitor of PKB-mediated insulin signalling in primary hepatocytes. The Biochemical journal. 2005;386:113-8.

Koh HJ, Toyoda T, Didesch MM, Lee MY, Sleeman MW, Kulkarni RN, Musi N, Hirshman MF, Goodyear LJ. Tribbles 3 mediates endoplasmic reticulum stress-induced insulin resistance in skeletal muscle. Nat Commun. 2013;4:1871.

Malhotra JD, Kaufman RJ. The endoplasmic reticulum and the unfolded protein response. Seminars in cell & developmental biology. 2007;18:716-31.

Ohoka N, Yoshii S, Hattori T, Onozaki K, Hayashi H. TRB3, a novel ER stress-inducible gene, is induced via ATF4-CHOP pathway and is involved in cell death. The EMBO journal. 2005;24:1243-55.

Ozcan U, Cao Q, Yilmaz E, Lee AH, Iwakoshi NN, Ozdelen E, Tuncman G, Gorgun C, Glimcher LH, Hotamisligil GS. Endoplasmic reticulum stress links obesity, insulin action, and type 2 diabetes. Science. 2004;306:457-61.

Ozcan U, Yilmaz E, Ozcan L, Furuhashi M, Vaillancourt E, Smith RO, Gorgun CZ, Hotamisligil GS. Chemical chaperones reduce ER stress and restore glucose homeostasis in a mouse model of type 2 diabetes. Science. 2006;313:1137-40.

Pal M, Wunderlich CM, Spohn G, Bronneke HS, Schmidt-Supprian M, Wunderlich FT. Alteration of JNK-1 signaling in skeletal muscle fails to affect glucose homeostasis and obesity-associated insulin resistance in mice. PloS one. 2013;8:e54247.

Pierre N, Barbe C, Gilson H, Deldicque L, Raymackers JM, Francaux M. Activation of ER stress by hydrogen peroxide in C2C12 myotubes. Biochem Biophys Res Commun. 2014;450:459-63.

Rieusset J, Chauvin MA, Durand A, Bravard A, Laugerette F, Michalski MC, Vidal H. Reduction of endoplasmic reticulum stress using chemical chaperones or Grp78 overexpression does not protect muscle cells from palmitate-induced insulin resistance. Biochem Biophys Res Commun. 2012;417:439-45.

Salvado L, Coll T, Gomez-Foix AM, Salmeron E, Barroso E, Palomer X, Vazquez-Carrera M. Oleate prevents saturated-fatty-acid-induced ER stress, inflammation and insulin resistance in skeletal muscle cells through an AMPK-dependent mechanism. Diabetologia. 2013;56:1372-82.

Urano F, Wang X, Bertolotti A, Zhang Y, Chung P, Harding HP, Ron D. Coupling of stress in the ER to activation of JNK protein kinases by transmembrane protein kinase IRE1. Science. 2000;287:664-6.

Vandesompele J, De Preter K, Pattyn F, Poppe B, Van Roy N, De Paepe A, Speleman F. Accurate normalization of real-time quantitative RT-PCR data by geometric averaging of multiple internal control genes. Genome biology. 2002;3:RESEARCH0034.

Vessby B, Uusitupa M, Hermansen K, Riccardi G, Rivellese AA, Tapsell LC, Nalsen C, Berglund L, Louheranta A, Rasmussen BM, Calvert GD, Maffetone A, Pedersen E, Gustafsson IB, Storlien LH. Substituting dietary saturated for monounsaturated fat impairs insulin sensitivity in healthy men and women: The KANWU Study. Diabetologia. 2001;44:312-9.

Yuzefovych L, Wilson G, Rachek L. Different effects of oleate vs. palmitate on mitochondrial function, apoptosis, and insulin signaling in L6 skeletal muscle cells: role of oxidative stress. American journal of physiology Endocrinology and metabolism. 2010;299:E1096-105.

Zhang K, Kaufman RJ. From endoplasmic-reticulum stress to the inflammatory response. Nature. 2008;454:455-62.

Zhang Y, Li F, Liu S, Wang H, Mahavadi S, Murthy KS, Khalili K, Hu W. MEKK1-MKK4-JNK-AP1 pathway negatively regulates Rgs4 expression in colonic smooth muscle cells. PLoS One. 2012;7:e35646.

Table 1. Sequences of primers (5'-3').

Genes	Forward	Reverse
ATF4	GAGCTTCCTGAACAGCGAAGTG	TGGCCACCTCCAGATAGTCATC
BiP	CTATTCCTGCGTCGGTGTGT	GCAAGAACTTGATGTCCTGCT
CHOP	CCTGAGGAGAGAGTGTTCCAG	CTCCTGCAGATCCTCATACCA
PPIA	CGTCTCCTTCGAGCTGTTTG	CCACCCTGGCACATGAATC
GRP94	GAGTCTCCCTGTGCTCTTGTG	TCTTCATCTTCCTTAATCCGCC
IRE1α	CAGTTTTTCCAGGATGTAAGTGACC	CAGTGATGTTCTCCCGCCAG
RPL4	CGCAACATCCCTGGTATTACT	TGTGCATGGGCAGGTTATAGT
RPL19	GAAGGTCAAAGGGAATGTGTTCA	CCTTGTCTGCCTTCAGCTTGT
TRB3	TGTGAGAGGACGAAGCTGGTG	TCGTGGAATGGGTATCTGCC
XBP1s	TGAGAACCAGGAGTTAAGAACACGC	CCTGCACCTGCTGCGGAC

ATF4: activating transcription factor 4, BiP: binding immunoglobulin protein, CHOP: C/EBP homologous protein, PPIA: peptidylprolyl isomerase A, GRP94: 94 kDa glucose-regulated protein, IRE1α: inositol-requiring 1α, RPL4: ribosomal protein L4, RPL19: ribosomal protein L19, TRB3: tribbles homolog 3, XBP1s: X-box-binding protein 1 spliced.

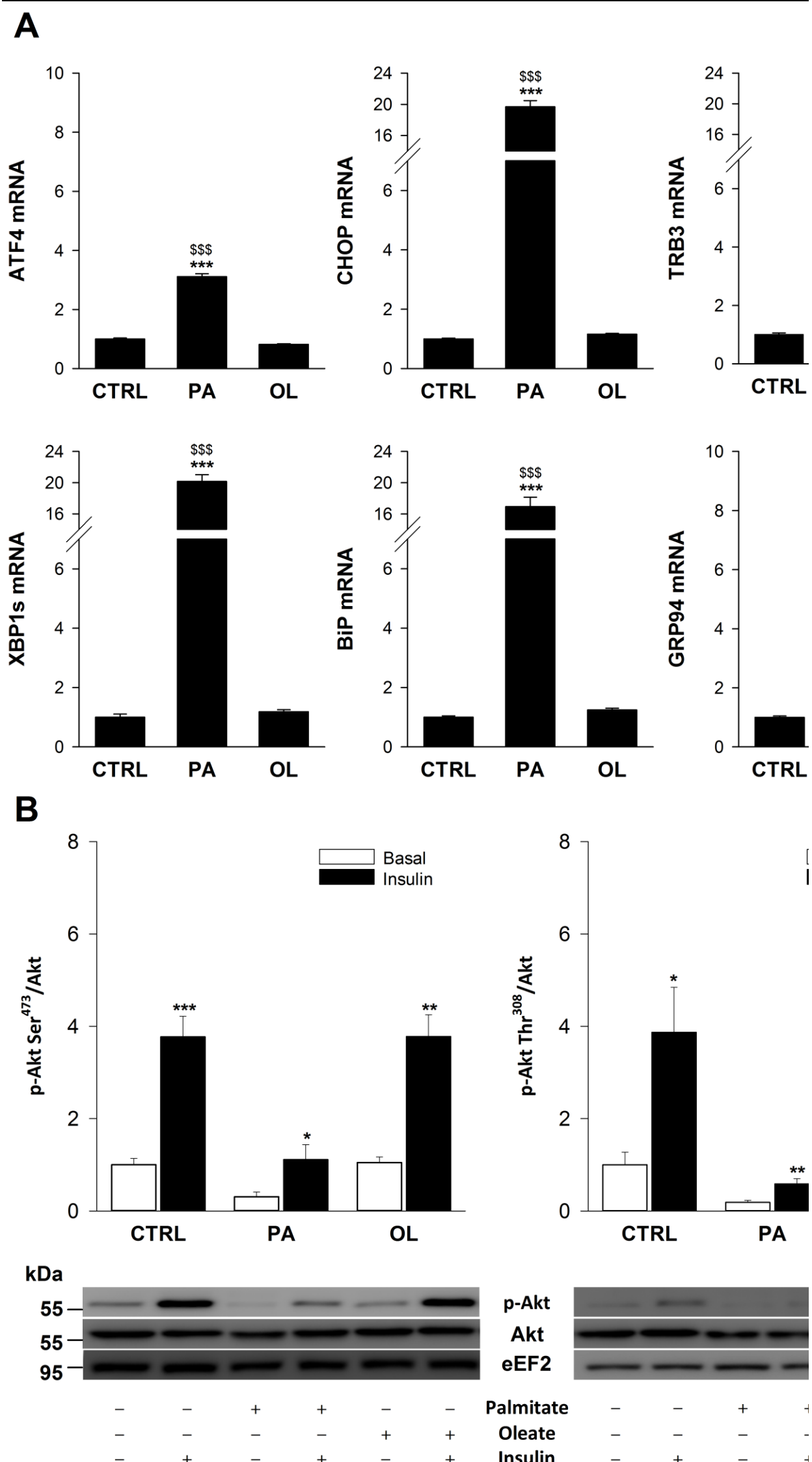
A
ATF4 mRNA
CHOP mRNA
TRB3 mRNA
XBP1s mRNA
BiP mRNA
GRP94 mRNA
$$$
***
CTRL
PA
OL
B
Basal
Insulin
p-Akt Ser473/Akt
p-Akt Thr308/Akt
kDa
55
55
95
p-Akt
Akt
eEF2
Palmitate
Oleate
Insulin

Figure 1. Palmitate induces ER stress and disrupts insulin signaling in C2C12 myotubes. (A) ATF4, CHOP, TRB3, XBP1s, BiP and GRP94 mRNA levels after 1 mM palmitate (PA) or oleate (OL) for 17 h. n=3; ***P<0.001 vs. CTRL; $^{\$\$\$}$P<0.001 vs. OL; one-way ANOVA with Bonferroni post-hoc test. (B) Phosphorylation state of Akt-Ser^{473} and Akt-Thr^{308} after 1 mM of palmitate or oleate for 17 h followed by insulin stimulation. n=3; *P<0.05, **P<0.01, ***P<0.001 vs. basal; unpaired t-test. All results are presented as means ± SEM.

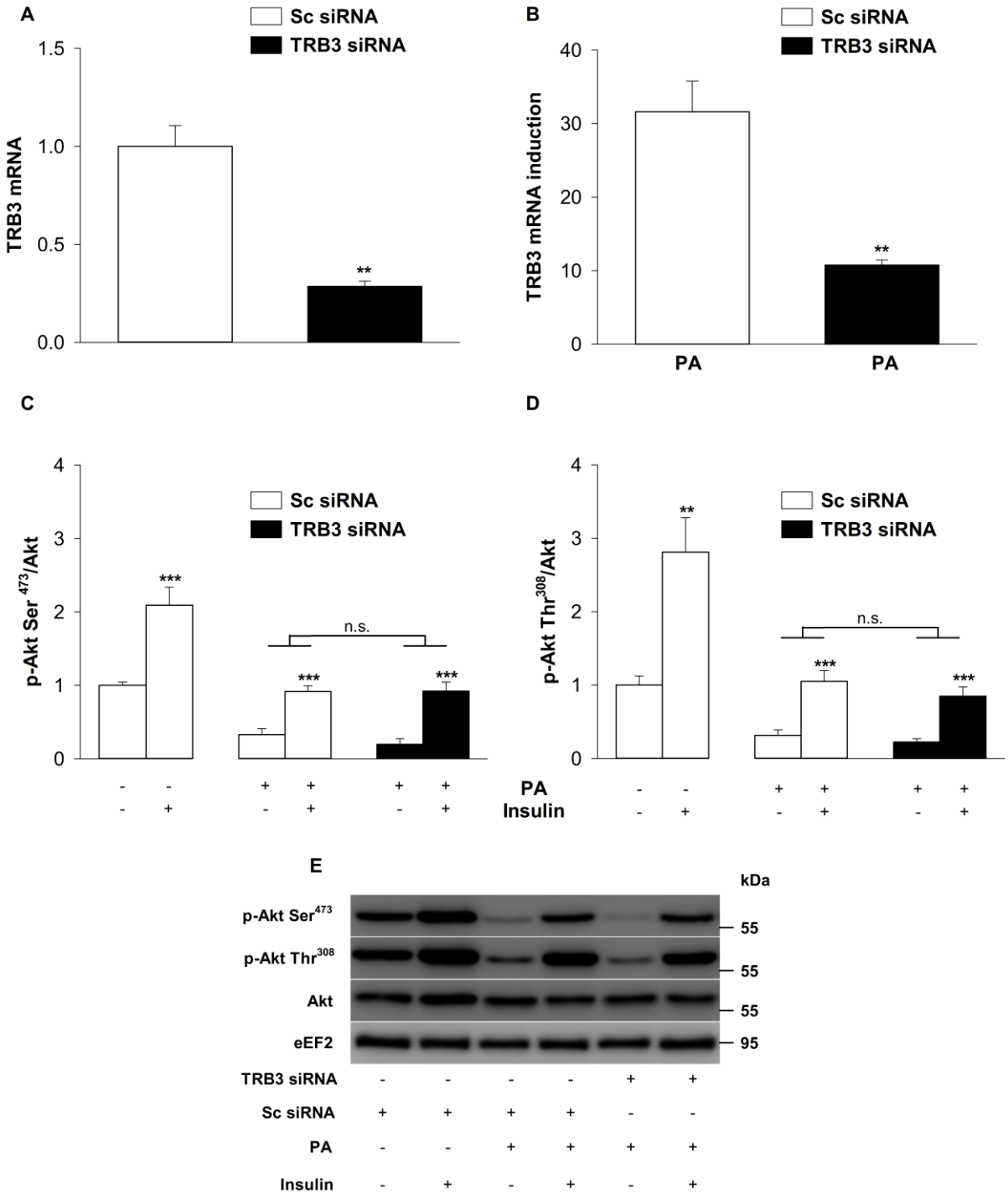

Figure 2. TRB3 does not contribute to palmitate-induced impairment of insulin signaling in C2C12 myotubes. (A) TRB3 mRNA level after transfection with either scramble (Sc) or TRB3 siRNA. Data correspond to one experiment run in triplicate; **P<0.01 vs. Sc siRNA; unpaired t-test. (B) TRB3 mRNA induction after 17 h palmitate (PA, 1 mM), with scramble or TRB3 siRNA. Data correspond to one experiment run in triplicate; **P<0.01 vs. Sc

siRNA; unpaired t-test. (C-D, left) Phosphorylation state of Akt-Ser^{473} and Akt-Thr^{308} after insulin stimulation in the presence of scramble siRNA. n=3; **P<0.01, ***P<0.001 vs. unstimulated condition; unpaired t-test. (C-D, right) Phosphorylation state of Akt-Ser^{473} and Akt-Thr^{308} after 17 h palmitate (1 mM) followed by insulin stimulation, in the presence of scramble or TRB3 siRNA. n=3; ***P<0.001 vs. unstimulated in the same transfection condition; n.s., non-significant; two-way ANOVA with Bonferroni post-hoc test. (E) Illustration of the data presented in C and D. All results are presented as means ± SEM.

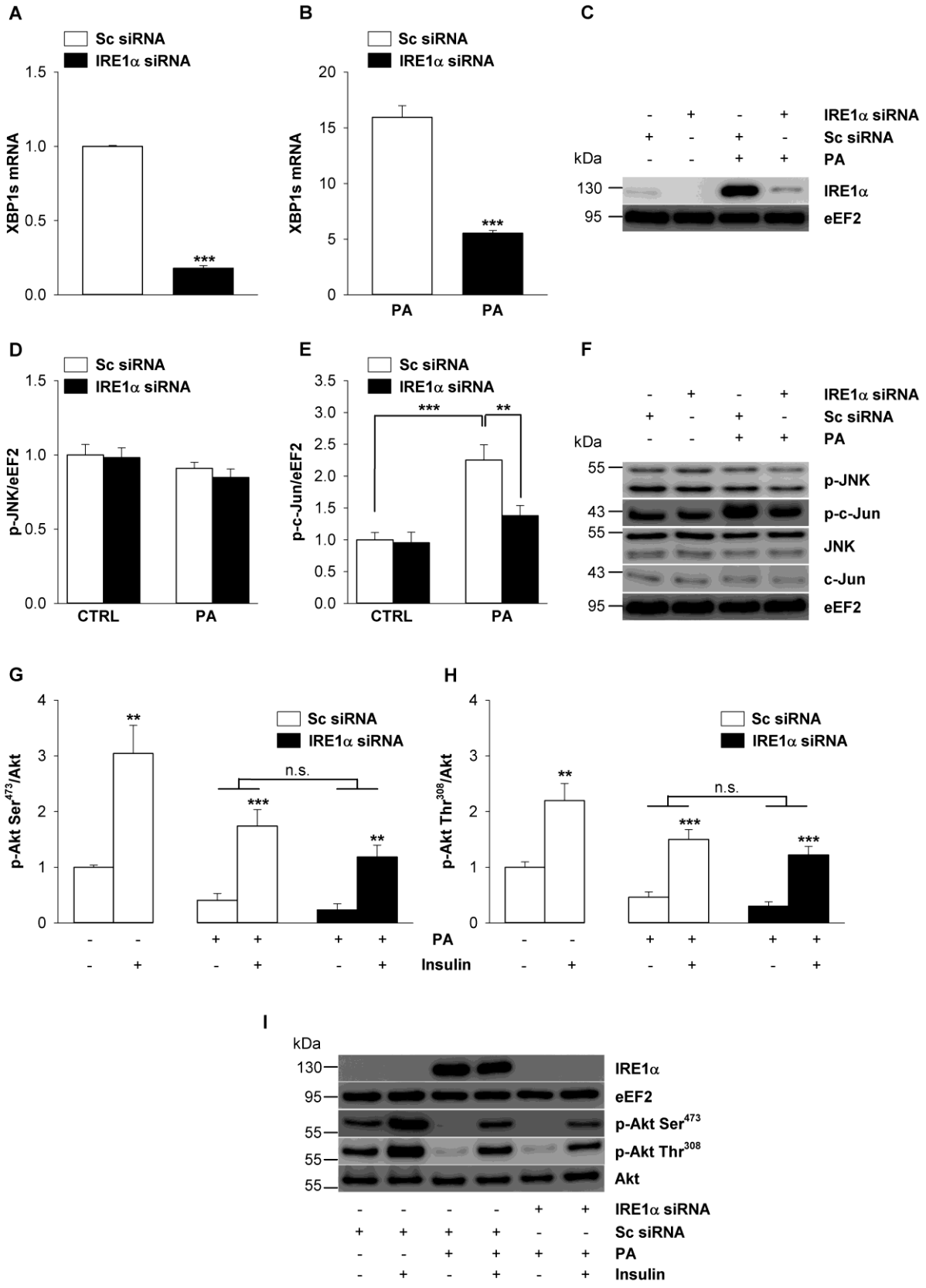

Figure 3. IRE1α does not participate in palmitate-induced impairment of insulin signaling in C2C12 myotubes. (A) XBP1s mRNA level after transfection with either scramble (Sc) or

IRE1α siRNA. Data correspond to one experiment run in triplicate. ***P<0.001 vs. Sc siRNA; unpaired t-test. (B) XBP1s mRNA level after 17 h of palmitate (PA, 1 mM), and in the presence of scramble (Sc) or IRE1α siRNA. Data correspond to one experiment run in triplicate. ***P<0.001 vs. Sc siRNA; unpaired t-test. (C) Representative western blot of IRE1α after 17 h of palmitate (PA, 1 mM), and in the presence of scramble (Sc) or IRE1α siRNA. (D-E) Phosphorylation state of JNK and c-Jun after 17 h palmitate (PA, 1 mM), with scramble (Sc) or IRE1α siRNA. n=3; ***P<0.001, **P<0.01; two-way ANOVA with Bonferroni post-hoc test. (F) Illustration of the data presented in A and B. (G-H, left) Phosphorylation state of Akt-Ser^{473} and Akt-Thr^{308} after insulin stimulation in the presence of scramble siRNA. n=3; **P<0.01 vs. unstimulated condition; unpaired t-test. (G-H, right) Phosphorylation state of Akt-Ser^{473} and Akt-Thr^{308} after 17 h palmitate followed by insulin stimulation, in the presence of scramble or IRE1α siRNA. n=3; **P<0.01, ***P<0.001 vs. unstimulated in the same transfection condition; n.s., non-significant; two-way ANOVA with Bonferroni post-hoc test. (I) Illustration of the data presented in G and H. All results are presented as means ± SEM.